Applied Materials Today 19 (2020) 100549

Contents lists available at ScienceDirect

Applied Materials Today

journal homepage: www.elsevier.com/locate/apmt

PVA-based peelable films loaded with tetraethylenepentamine for the removal of corrosion products from bronze

Teresa Guaragnone, Andrea Casini, David Chelazzi*, Rodorico Giorgi*

University of Florence, Department of Chemistry "Ugo Schiff" and CSGI, Via della Lastruccia 3, 50019 Sesto Fiorentino, Italy

ARTICLE INFO

Article history:
Received 18 October 2019
Received in revised form
19 December 2019
Accepted 25 December 2019

Keywords:
Bronze
Peelable films
HVPDs
PVA
Tetraethylenepentamine
Corrosion patina

ABSTRACT

The removal of corrosion products from bronze artifacts is still an open challenge, in particular when stubborn corrosion patinas are found on surfaces with pronounced cavities and reliefs. Highly viscous polymeric dispersions (HVPDs) of polyvinyl alcohol (PVA) are able to adhere to highly textured 3D surfaces, forming films that can be easily peeled off. Here, PVA-based HVPDs were loaded with tetraethylenepentamine (TEPA), whose copper(II) complex has a stability constant four orders of magnitude higher than that of EDTA tetrasodium salt, traditionally used by conservators for cleaning bronze. TEPA promotes alkaline hydrolysis of acetyl groups in PVA, leading to the association of the polymer chains into more ordered structures, reducing significantly the time needed for the formation of films as compared to HVPDs loaded with water. Besides, the solubility of TEPA in most polar solvents allows to upload higher quantities of chelating agent in the HVPD, as opposed to EDTA. The confinement of TEPA inside the PVA matrix allowed the effective and progressive removal of copper corrosion products from a 16th century Italian bronze masterpiece, preserving the natural cuprite patina of the historical bronze, in times drastically shorter than traditional cleaning methods.

1. Introduction

The preservation of metal artifacts is an open challenge in conservation science, owing to the severe degradation processes (such as the so-called "bronze disease" [1]) that affect metallic sculptures and objects belonging to different artistic productions and ages [2]. In particular, the removal of corrosion patinas from bronze is risky and time-consuming when carried out with traditional methods. Both dry mechanical (brushes, scalpels, chisels) and wet cleaning with non-confined solvents and solutions, are invasive and scarcely controllable, potentially causing damage to the artifacts [3]. Laser ablation can grant fast cleaning action, but can lead to heating processes on the surface [4]. Alternatively, wet cleaning shows enhanced efficacy and non-invasiveness when solvents or solutions are confined in retentive matrices able to gradually release the cleaning fluids on sensitive surfaces. Besides, confined fluids have reduced volatility, which strongly decreases the health issues related to the use of solvents in art conservation [3].

Chemical and physical gels have proved to be optimal confining matrices for cleaning fluids, and in the last decades polymers such as poly(2-hydroxyethyl methacrylate) (pHEMA), polyvinyl pyrrolidone (PVP) and polyvinyl alcohol (PVA) have been employed to formulate systems with ideal mechanical properties and retentiveness [5–9]. In particular, both gels and highly viscous polymeric dispersions (HVPDs) have been widely employed; the first are characterized by the presence of polymer networks physically or chemically cross-linked, with rheological properties that resemble those of solids (e.g. highly viscoelastic, with storage modulus higher than loss modulus over the whole frequency span as measured in oscillatory frequency sweeps [10]). Hydrogels are able to upload aqueous solutions and, to some extent, polar solvents, as opposed to organogels that are used to confine average- or low-polarity solvents [11]. HVPDs comprise polymer dispersions or solutions that do not exhibit the aforementioned rheological behavior and are mainly used as thickeners to limit the diffusion of cleaning fluids. Typically, hydrogels are prepared as sheets with a thickness of few millimeters, whose elasticity can be tuned changing the type of polymer and the synthetic process. These systems allowed the treatment of flat surfaces and contemporary painted layers with 3D texture [12]. However bronze sculptures usually exhibit highly textured surfaces with pronounced cavities and reliefs that are hardly accessible with the aforementioned formulations. PVA-based highly viscous polymeric dispersions (HVPDs) are able to homogeneously cover highly rough surfaces, and after application

* Corresponding authors.
E-mail addresses: chelazzi@csgi.unifi.it (D. Chelazzi), rodorico.giorgi@unifi.it (R. Giorgi).

https://doi.org/10.1016/j.apmt.2019.100549
2352-9407/

Table 1
Composition (w/w %) of the polymer dispersion. ES = loaded with an aqueous solution of EDTA (0.5 M); TS = loaded with an aqueous solution of TEPA (0.5 M); T = loaded with TEPA.

Name	PVA	H_2O	EtOH	DPG	MPD	GLY	PEG	EDTA 0.5 M	TEPA 0.5 M	TEPA
PVA	20	57	17	2.5	2.5	0.6	0.4	–	–	–
PVA_{ES}	20	54	17	2.5	2.5	0.6	0.4	3	–	–
PVA_{TS}	20	54	17	2.5	2.5	0.6	0.4	–	3	–
PVA_{T}	20	54	17	2.5	2.5	0.6	0.4	–	–	3

they can be easily removed in one piece thanks to their viscoelasticity [13]. PVA has excellent chemical stability, biocompatibility, low toxicity and cost, and good film forming properties [14–16]. The characteristics of the films can be tuned by adding solvents and plasticizers to the formulation, for instance ethanol has a structuring effect on water, and thus increases the order of the structure of the polymeric network [9,13]. The adhesion of these films onto the substrate can be such that decohered and detached layers are peeled along with the film. This feature is particularly appealing when treating metal substrates, whose cohesive forces are typically much stronger than those of superficial corrosion layers [17].

Initially, HVPDs formulated for the cleaning of bronze were applied as loaded with an aqueous solution of ethylenediaminetetraacetic acid disodium salt dihydrate (Na_2EDTA) [17], a traditional chelating agent widely used for the removal of copper corrosion products [18]. Despite the good stability of EDTA-copper(II) complexes, it is not uncommon to find stubborn corrosion layers that are resistant to treatments with EDTA. Indeed, obtaining a safe, fast and effective removal of degradation products from bronze artifacts is still an open issue in art conservation. A valid alternative to EDTA is represented by tetraethylenepentamine (TEPA), whose copper(II) complex has a stability constant ($\log K_f = 22.8$ at 25 °C) four orders of magnitude higher than that of EDTA tetrasodium salt (Y^{4-}, $\log K_f = 18.8$ at 25 °C) [19]. The use of TEPA, properly confined in retentive matrices, is thus expected to enhance cleaning efficacy, with unprecedented results.

Moreover, EDTA is poorly soluble in ethanol, and it was shown that only limited amounts of Na_2EDTA can be uploaded in the water-ethanol blend contained in the PVA-based HVPDs before phase separation occurs [17]. Instead, TEPA has high solubility in most polar solvents [20], which allows the upload of larger quantities of chelating agent in the dispersion, likely boosting the removal of corrosion products.

In this contribution, we formulated PVA-based HVPDs loaded with TEPA, and studied how the presence of the polyamine affects the film forming process and the physico-chemical properties of the films. In fact, diethyleneamines are usually employed as crosslinking agents of PVA, and are expected to modify the interactions among the polymer chains [21]. The HVPDs and the filmed dispersions were characterized through differential scanning calorimetry (DSC), rheological measurements, attenuated total reflectance Fourier transform infrared spectroscopy (ATR-FTIR) and field emission gun scanning electron microscopy (FEG-SEM) coupled with energy-dispersive X-ray analysis (EDX). The HVPDs were then applied onto corroded bronze mock-ups, and the removal of corrosion patinas was checked at the micron scale with 2D Imaging FTIR, using a Focal Plane Array (FPA) detector. Finally, a selected HVPD formulation was used to remove stubborn corrosion layers from a 16th century bronze masterpiece by Benvenuto Cellini.

2. Materials and methods

2.1. Materials

Poly(vinyl alcohol) [PVA] (87–89% hydrolyzed, Mw 85,000–124,000, DP ≈ 2000, cps 23.0–27.0, Aldrich), dipropylene glycol [DPG] (99%, mixture of isomers, Aldrich), 2-methyl-1,3-propanediol [MPD] (99%, Aldrich), glycerol [GLY] (analytical grade, Merck), polyethylene glycol [PEG] (average Mn 300), ethanol [EtOH] (purity ≥98%, Fluka), ethylenediaminetetraacetic acid disodium salt dihydrate [Na_2EDTA] (>99.9%, Aldrich), NH_4OH solution (30–33% NH_3, Sigma-Aldrich), tetraethylenepentamine [TEPA] (technical grade, Aldrich), hydrochloric acid (37%, Sigma), copper(II) chloride dihydrate (>99.9%, Sigma), sodium chloride (≥99.0%, Aldrich), and sodium hydroxide (98.5%, for analysis, pellets, Acros Organics), were used as purchased. Water was purified by a Millipore MilliRO-6 Milli-Q gradient system (resistivity >18 MΩ cm).

2.2. HVPDs preparation

A polymeric dispersion (20% w/w) was prepared by dissolving PVA powder into purified water at 90 °C for 2 h, in a three-neck flask equipped with a condenser to avoid water evaporation during heating. Once the polymer solubilization was completely achieved, the temperature was decreased to 70 °C and plasticizers (PEG, DPG, MPD, GLY) were added (see Table 1). After 30 min, ethanol was added (17% w/w), and the final system was sonicated for 1 h in pulsed mode at 55 °C until a transparent polymeric dispersion was obtained. The synthesis was carried out under continuous stirring at 150 rpm with a stirring paddle, to reach and maintain the correct homogenization. The pH of the HVPD, measured with an indicator paper, was 6.5 ± 0.5.

2.3. Complexing agents addition

The upload of EDTA was carried out as follows. A 0.5 M EDTA aqueous solution (pH 8.5) was added to the PVA solution under stirring, after the solubilization of PVA and the addition of plasticizers, but before the addition of ethanol, so as to avoid the precipitation of the salt. The EDTA solution corresponds to 3% (w/w) of the total weight of the HVPD (see Table 1); similar concentration values are typically used in the bronze restoration practice [17]. Adding more EDTA solution to the HVPD results in a phase separation and sedimentation of Na_2EDTA [17]. The pH was then adjusted to 9 ± 0.5 by addition of few droplets of a concentrated (33%) ammonia solution.

Loading with TEPA was carried out by adding a 0.5 M solution of TEPA (3% w/w) to the HVPD (see Table 1). The final pH was 8.2 ± 0.2. For application onto stubborn corrosion patinas on the real bronze artifact, the loading was carried out by direct addition of TEPA (as received from the supplier) to the polymeric dispersion (3% w/w), and subsequent stirring with a vortex at 2400 rpm, until the amine was completely dissolved. The final pH is strongly alkaline.

It is worth noticing that, even though the volatility and dispersibility (and hence the risk exposure) of fluids is decreased once they are confined in polymeric networks [11], the health and environmental issues involved in the handling and disposal of TEPA-loaded dispersions/films must be considered. The standard safety measures can be adopted for handling these systems (e.g. use of laboratory gloves and goggles), and for their disposal.

2.4. Physico-chemical characterization

Studies of the evaporation kinetics of the volatile fraction (water and ethanol) contained in the HVPDs were carried out by gravimetric measurements. To simulate the process of film formation in real conditions, 0.5 g of each formulation was applied on microscope glass slides and spread with a spatula over an area of 2.5 × 2.5 cm^2 to obtain a thickness of about 0.2 mm. Five samples were prepared for each HVPD system, and one sample for each HVPD type was periodically weighted for 5 h to control the evaporation process at 25 °C and 45% RH. The other 4 slides were let dry in the same conditions until the film could be easily removed with tweezers from the glass without disrupting it or leaving residues. At this point in the evaporation process the films were thus deemed to be peelable. The loss of volatile fraction as a function of time was calculated according to the following equation:

$$W_{vf} = \frac{W_t - W_d}{W_i - W_d} \cdot 100$$

where W_{vf} is the volatile fraction loss, W_t is the weight of the film at given time t, W_d and W_i are, respectively, the final dry weight and the initial weight of the film. Weight measurements were repeated twice.

Changes in viscoelastic behavior as a function of time during drying were investigated by means of oscillatory shear measurements performed on formulations with and without TEPA. Oscillatory tests were performed using a Discovery HR-3 rheometer from TA Instruments equipped with a parallel plate geometry of 25 mm diameter and a Peltier temperature control system (all measurements were carried out at 25.0 ± 1 °C). The gap was adjusted in order to obtain a maximum normal force of 0.9 N. Fluid samples were continuously kept under manual stirring in order to maintain the homogeneity of the systems. Film samples were prepared by pouring 11 g of the polymeric dispersion into a Petri dish, and then the dispersions were equilibrated for 2 days at 25 °C and 55% RH. Frequency sweep measurements were carried out within the linear viscoelastic range (5% strain) determined by previous amplitude sweep tests. The storage (G′) and loss (G″) moduli were measured over the frequency range 0.01–100 Hz.

The thermal properties of the dried films were determined by DSC on a TA Instruments (Q2000) apparatus. The films were cast as specified above, peeled from glass slides, and let dry overnight at room temperature. Then, the films were dried at 40 °C for 48 h in an oven. The films were placed in sealed steel pans and heated with a heating rate of 10 °C/min, under nitrogen flow (50 mL/min). First, an annealing cycle was carried out, heating the films up to 250 °C. Then, the films were cooled to 25 °C and re-heated to 250 °C. Glass transition (T_g) and melting temperatures (T_m) were obtained from the thermal curves after the second heating cycle, and the enthalpy of fusion (ΔH_m) was obtained from the integrated area of the melting peak. Each measurement was repeated 3 times. The degree of crystallinity (DC%) was determined using the equation:

$$DC\% = \frac{\Delta H_m}{\Delta H_{100}} \cdot 100$$

where ΔH_m is the measured melting enthalpy and ΔH_{100} is the melting enthalpy of a completely crystalline PVA (ΔH_{100} = 138.6 J/g) [22].

Morphological features of the HVPD films and of the artificially aged bronze samples were studied by SEM analysis performed using a Field Emission Gun Scanning Electron Microscope SIGMA (FEG-SEM, Carl Zeiss Microscopy GmbH, Germany), using an acceleration potential of 3 kV and a 3.9 mm working distance. Prior to SEM analysis, films were prepared as for the DSC measurements, and metallized with gold using an Agar Scientific Auto Sputter Coater. The bronze mock-up (coin) was analyzed without gold sputtering.

Elemental analysis was conducted with EDX associated to the SEM apparatus. The X-ray counts were obtained by integrating Kα X-ray peaks using an Oxford Instruments INCA X-act microanalyzer.

ATR-FTIR analysis was carried out on dry films using a Thermo Nicolet Nexus 870 with an MCT detector (Mercury Cadmium Tellurium). The spectra were recorded between 650 cm^{-1} and 4000 cm^{-1}, with a spectral resolution of 4 cm^{-1} and 128 scans for each spectrum.

FTIR analysis on bronze mockups was carried out using a Cary 620–670 FTIR microscope (Agilent Technologies). Measurements were performed using a Focal Plane Array (FPA) 128 × 128 detector, which allows the highest spatial resolution currently available to FTIR microscopes. The spectra were recorded directly on the surface of the samples (corroded bronze mock-ups, or the Au background) in reflectance mode, with open aperture and a spectral resolution of 8 cm^{-1}, acquiring 128 scans for each spectrum. The spectral range was 4000–900 cm^{-1}. The FPA detector was used to perform 2D FTIR imaging. A "single-tile" analysis results in a map of 700 × 700 mm^2 (128 × 128 pixels), and the spatial resolution of each imaging map is 5.5 mm (i.e. each pixel has dimensions of 5.5 × 5.5 mm^2). Multiple tiles were acquired to form mosaics.

2.5. Artificially aged samples

A bronze coin was provided by CNR-ISMN (Rome). The chemical composition mimics that of bronze coins typical of the classic Roman period and was assumed to be a standard for classic bronze artifacts. The composition of the coin is as follows: Cu 92.3 wt%, Sn 7.5 wt%, Pb 0.2 wt% [23]. The coin was treated mechanically with sanding paper to increase its surface roughness, so as to favor the formation and adhesion of degradation products during accelerated aging. The aging protocol for the production of artificial patinas containing copper(II) chlorides was carried out as reported elsewhere [24].

2.6. Cleaning procedure

The HVPDs were applied directly on bronze surfaces, lying down 0.25 g on 20 mm^2. The HVPDs were let dry and film for 1.5 h, and then were peeled off the surface using tweezers. The same application protocol was followed on a real bronze artifact (16th century bronze bas-relief by Benvenuto Cellini).

3. Results and discussion

HVPDs loaded with TEPA appear yellowish and more viscous than transparent dispersions loaded with water. Besides, films cast from TEPA-containing HVPDs seem to have a more pronounced elastic behavior. Gravimetric and rheological measurements quantified the effect of the addition of TEPA on the film-forming process and on the viscoelastic properties of dispersions and films. Fig. 1 shows the loss of volatile fraction, i.e. water and ethanol, over time from HVPDs loaded either with water or with TEPA. In the plots, we marked the points in time when the films are easily peeled off the glass slide surface. Loading with TEPA (0.5 M, 3% w/w) reduces the time needed for the formation of peelable films down to ca. 100 min, i.e. half the time needed when the HVPD is loaded with water (pH 6.5). When film formation occurs, the TEPA-containing system has the highest liquid content, and still contains a liquid fraction after 300 min, when the water-loaded system is completely dry. We ascribed the reduced volatility in the presence of TEPA both to the earlier formation of a surface film that limits evaporation, and to the high boiling point of TEPA (340 °C when pure).

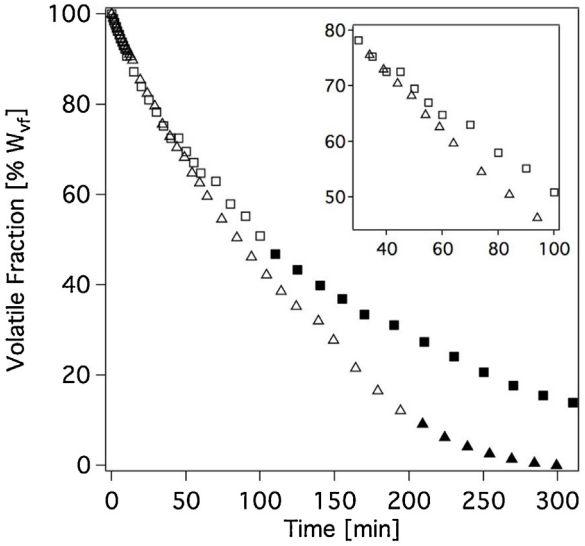

Fig. 1. Loss of volatile fraction (water, ethanol) over time, from PVA-based HVPDs loaded with water (triangles) or TEPA (3% w/w; squares). Full markers indicate the time span, up to 300 min, where films could be easily peeled off the surface in one piece; the first full marker can be thus assumed as the time of film formation. The inset highlights the first 100 min of volatile fraction loss.

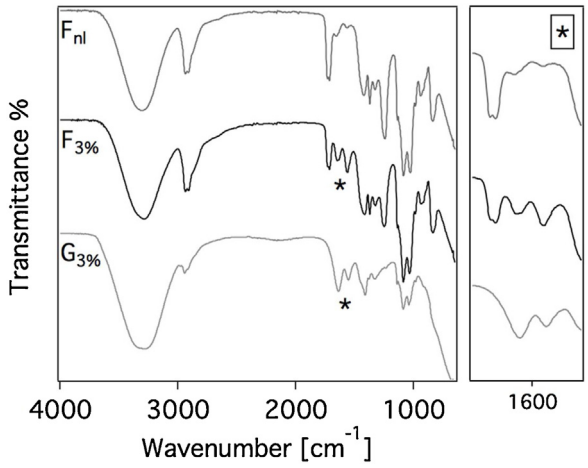

Fig. 2. ATR spectra of films cast from PVA-based HVPDs loaded with water (F_{nl}), or loaded with TEPA 3% (F3%). The spectrum of the gum formed ca. 1 week after the addition of TEPA (G3%) is also showed. Moving from F_{nl} to G3% it is possible to observe the appearance of bands at 1643 (N—H deformation of -NH_3^+ groups in the partially protonated TEPA) and 1564 cm^{-1} (carbonyl stretching of acetate ions formed by the alkaline hydrolysis of polyvinyl acetate groups in PVA), and the corresponding disappearance of the acetate C=O stretching peak (1716 cm^{-1}) (see also the inset).

Overall, gravimetric measurements suggest that the high alkalinity of the TEPA solution favors the interactions between PVA chains, resulting in earlier film formation than for water-loaded HVPDs. In fact, Hebeish et al. reported that sodium hydroxide solutions at high pH cause significant hydrolysis of the acetyl groups of PVA, increasing the tendency of PVA molecules to associate, and thus enhancing the viscosity of the PVA dispersions [25]. We verified that, when the HVPDs are loaded with solutions of NaOH (pH 14), they turn into highly elastic, solid-like gums already within one minute, which prevented gravimetric and rheological measurements on those systems. The transformation is thermally irreversible. Such a fast viscosity increase prevents any practical application, as the gums are too rigid and retentive to be used for cleaning purposes. Interestingly, in the presence of TEPA the formation of the gum is much slower (e.g. 1 week) even at high pH values, making the application of TEPA-loaded HVPDs feasible. The HVPD loaded with water at pH 6.5 is stable for long time (e.g. one year) if stored in sealed vials.

The ATR spectra of the films loaded with water show the typical absorptions of poly(vinyl alcohol) at 3300 (—OH stretching), 2934 and 2914 (C—H stretching), 1718 (C=O stretching of the acetate carbonyl group), 1143 and 1088 cm^{-1} (C—O stretching in PVA) [26]. In the spectra of the TEPA-containing HVPDs, the bands at 1643 and 1564 cm^{-1} are assigned respectively to the N—H deformation of —NH_3^+ groups in the partially protonated TEPA molecules [27], and to the carbonyl stretching of acetate ions formed by the alkaline hydrolysis of polyvinyl acetate groups in PVA [28]. The intensity of the carbonyl peak of non-hydrolyzed acetate groups (1718 cm^{-1}) decreases accordingly, and the peak is no longer observable in the spectra of the gum, which show a marked increase of the band of protonated TEPA at 1643 cm^{-1}.

Partly protonated polyamines are able to interact with acetate ions, and the formed ionic couples might hinder (e.g. through steric hindrance) the association of PVA chains, slowing down the process that turns the HVPDs into gums (Fig. 2).

Morphological analysis by SEM showed that the cross-section of the films loaded with water (Fig. 3A) exhibit pores with diameters ranging from 1 to 20 μm, oriented along axes normal to the film surface. The majority of the pores are found in the lower layers, closer to the base surface of the film; instead, towards the upper surface, the film bulk becomes more compact and the pores turn into elongated channels with a section of few microns. This structure could be due to the rapid evaporation rate at the upper surface in the first minutes after the film is cast, leading to the collapse of porous structure closer to the top layers. The presence of micron-sized pores in the lower part of the film is expected to help the migration of dissolved degradation products from the film-patina interface into the

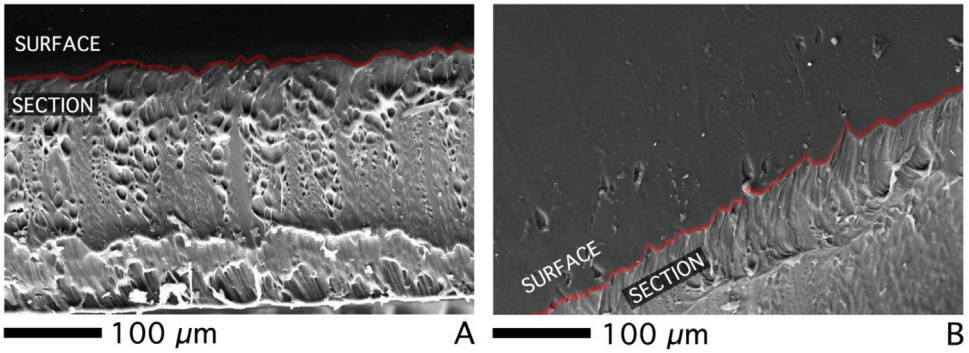

Fig. 3. SEM images of films cast from PVA-based HVPDs loaded with water (A) or with TEPA 3% wt (B). Panel A shows a cross-section of a film, while panel B shows the edge between the upper surface of a film (smooth dark grey area, top left part of the image) and the underlying layers (bottom right portion of the image).

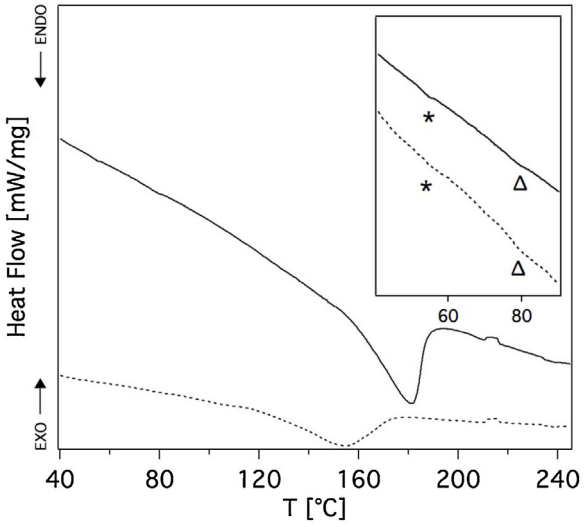

Fig. 4. DSC curves of films cast from PVA-based HVPDs loaded with water (broken line) or with TEPA (3% w/w; full line). The inset highlights the 50–90 °C region, showing the glass transition temperatures of PVA at ca. 55 °C (*) and 80 °C (Δ).

film's bulk, favoring the removal of degradation products. No significant differences were observed in the pore structure of films cast from HVPDs loaded with TEPA, as highlighted in Fig. 3B, where the bottom right portion of the image shows the underlying film layers beneath the surface. The surface of the films is smooth, with no observable porosity (see Fig. 3B, smooth dark grey area in the top left part of the image).

Further information was gained by thermal analysis. The degree of crystallinity of the films loaded with water, in the presence of plasticizers (PEG, DPG, MPD, GLY), is 10.60%, i.e. lower than that of films obtained with the same quantity of PVA (of the same type) simply loaded with water (DC% = 12.80% [29]). As expected, the presence of plasticizers weakens the secondary bonds between the PVA chains, decreasing the crystallinity. However, when TEPA is added to the formulation, the films DC% raises to ca. 15%. Besides, the melting temperature of PVA increases from 155 ± 2 °C to 177 ± 7 °C, closer to the melting of fully hydrolyzed PVA (230 °C [30]). The melting peak becomes narrower, consistently with the crystallinity increase (see Fig. 4). This behavior supports the hypothesis that the hydrolysis of PVA acetyl groups in the alkaline environment provided by the TEPA solution, favors the association of the polymer chains into more ordered structures. The amorphous regions in the films exhibit similar glass transition temperatures (T_g, see inset in Fig. 4) regardless the type of solution loaded (water or TEPA); in both cases two transitions are observed at ca. 55 °C and 80 °C. The first one is the less intense and is close to the T_g of polyvinyl acetate, while the second is assigned to PVA with a low degree of hydrolysis [31].

The rheological behavior of the HVPDs (oscillatory frequency sweeps), is shown in Fig. 5. Essentially, the dispersions initially behave as viscous fluids, with a loss modulus (G") higher than the storage modulus (G') over the whole frequency span. After the dispersions are cast, the film formation process results in an increase of both G' and G", and the cross-over point (i.e. the point in frequency sweeps where the G' and G" curves meet) recedes to lower oscillation frequencies, indicating that the dispersions become more "solid-like" as the films form. When the dispersions are loaded with TEPA, the whole process is faster, in agreement with the information obtained from the other techniques.

In conclusion, based on the physico-chemical characterization discussed in the previous paragraphs, the TEPA-loaded HVPD was deemed as a good candidate for cleaning tests on corroded bronze mock-ups (coins), before application on a real bronze artifact. Fig. 6 shows the treatment of a bronze coin that exhibits corrosion patinas after accelerated aging. In all cases, ten applications were made for each type of HVPD (i.e. loaded with water, EDTA, or TEPA). In this case, loading the HVPD with low concentrations of chelating agents (0.5 M) did not produce satisfactory removal of the highly stubborn patinas, even though some slight removal was achieved with the TEPA-loaded HVPD as opposed to EDTA. Closer to the border of the coin, the patinas were less strongly adhered and cohered, so that peeling action upon film removal was enough to partially detach them even with the water-loaded dispersion. Complete removal of the patinas was instead obtained using the HVPD loaded with pure TEPA (3% w/w). As a matter of fact, the possibility of uploading higher quantities of chelating agent represents a fundamental applicative advantage of the TEPA-loaded HVPDs over EDTA. It must be noticed that Fig. 6 shows the final cleaning results after all the applications were carried out; however, the removal of the corrosion products was gradual and controllable, which is an important feature in real case studies where patinas need to be progressively thinned to avoid the removal of desired layers (e.g. cuprite [24]).

2D FTIR Imaging with an FPA detector allowed checking the removal of corrosion products down to the micron-scale, with a spatial resolution of 5.5 μm. Before cleaning, the spectra collected on the coin surface show intense hydroxyl stretching bands of hydrated copper(II) hydroxychlorides such as atacamite/clinoatacamite, at 3467, 3339, 3245, and 3154 cm^{-1} [32], as evidenced by the presence of red pixels in the FTIR 2D maps in Fig. 7. These corrosion products are particularly detrimental [33], as they are typically involved in the "bronze disease", a cyclic process that leads to the complete consumption of the metal layers [1]. Less intense bands at 1489, 1461, 1451 and 1385 cm^{-1} are ascribable to the presence of copper carbonates (azurite and malachite) [34]. After the application, the bronze metal surface is brought back (blue pixels in the maps). Besides, no traces of PVA were detected on the treated surface, down to the detection limit of the detector (<1 pg/pixel, 1 pixel = 30.25 μm^2). SEM-EDX confirmed that chlorine-containing patinas were efficiently removed following the application of the HVPDs loaded with the polyamine solution (see Fig. 8).

HVPDs loaded with TEPA (3% w/w) were then used to remove corrosion patinas from a 16th century bronze pedestal by Benvenuto Cellini, belonging to the Bargello National Museum of Florence (Italy). The pedestal is a bas-relief that represents the classic myth of Perseus rescuing Andromeda from a sea-monster. Greenish bronze degradation products had accumulated through centuries all around the three-dimensional figures, and in the cavities of the monster's scales, skin, eyes and ears, jeopardizing the visual aspect of the sculpture (see Fig. 9). The patinas were stubborn and resistant to EDTA (either confined in the HVPDs or not), and the only traditional approach left was dry mechanical cleaning, a time-consuming process that needs great care to avoid damaging the bronze layer underneath the corrosion products. Instead, the application of the HVPDs led to the feasible and controlled removal of the greenish corrosion layers, preserving the underlying reddish layer of cuprite (Cu_2O) [2,24,35] that conservators typically wish to maintain, as it passivates the metal against recurring corrosion. A crucial factor that made the intervention feasible was the ability of the HVPDs to penetrate cavities, adhering homogeneously to the surface, and filming into foils that were easily peeled off using tweezers, after solubilization and absorption of the Cu(II) degradation products. During the application, the strong blue discoloration of the films (see Fig. 9A,B) indicates the formation of the TEPA-copper(II) complex, and such a visual change is advantageous, as it permits to macroscopically follow the solubilization and removal of the corrosion layers from the bronze surface [36]. Overall, the use of the TEPA-loaded HVPDs allowed recovering the aestheti-

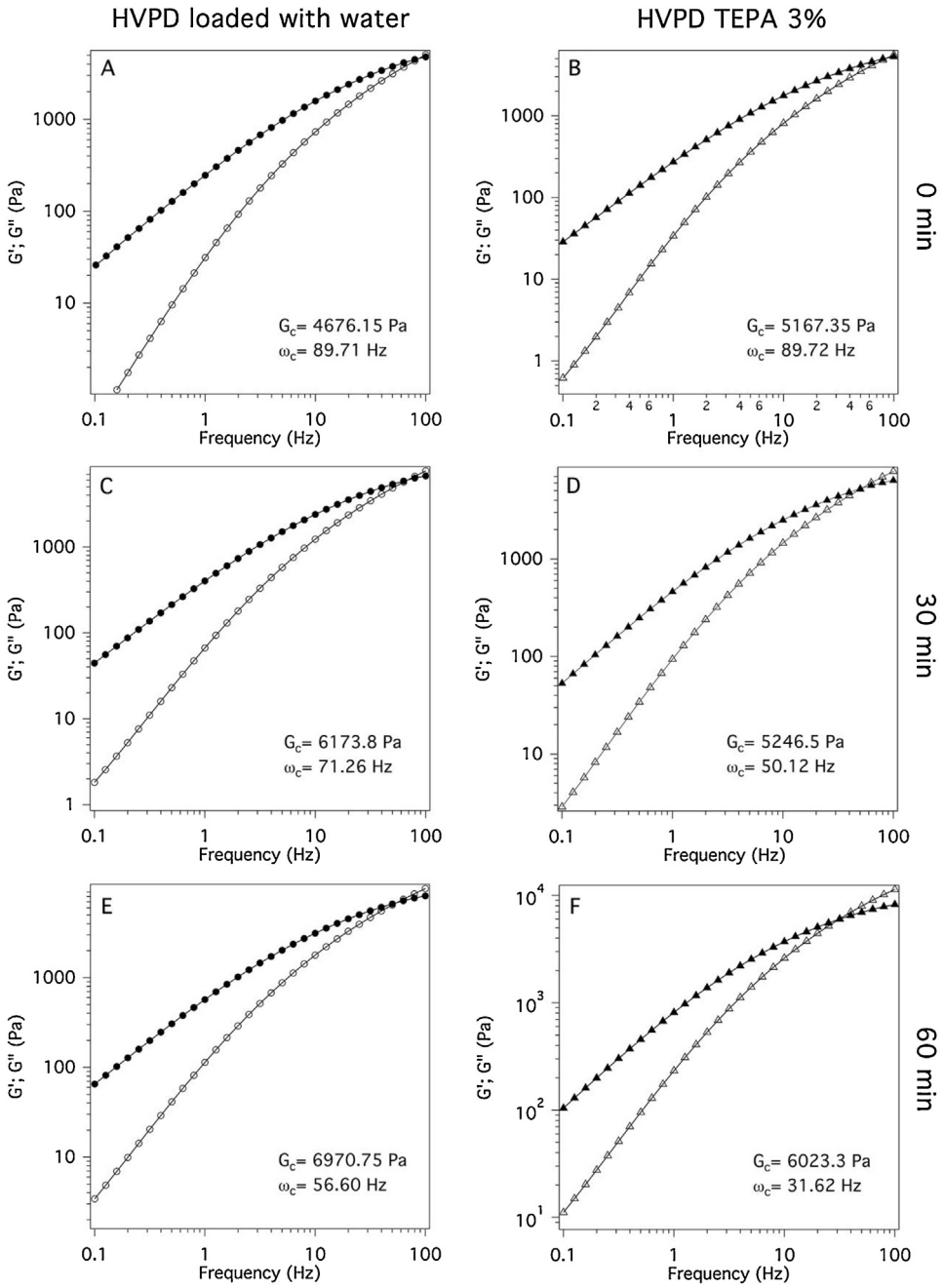

Fig. 5. Frequency sweeps (strain of 5%) of PVA-based HVPDs loaded with water and with TEPA (3 wt %), measured at different times after the films were cast. Open and closed markers represent G' and G", respectively.

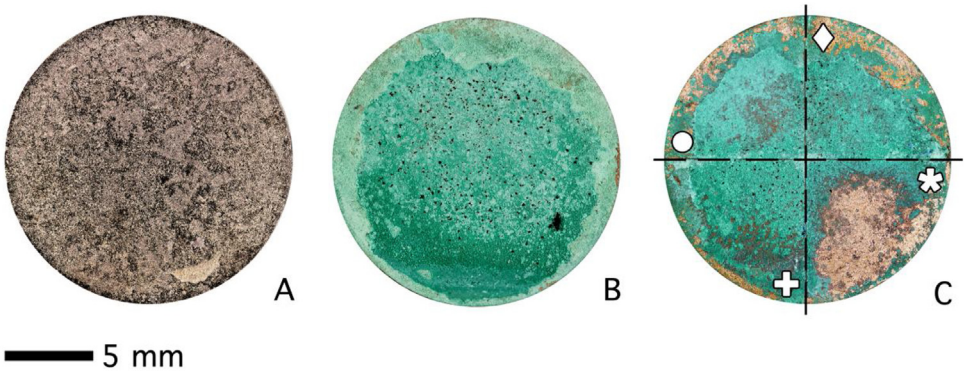

Fig. 6. Macro photography of the bronze coin mock-up before artificial aging (A), after artificial aging (B), and after the application of PVA HVPDs (C) loaded with water (+), TEPA 0.5 M 3% wt (•), EDTA 0.5 M 3% wt (♦), and TEPA 3% wt (*).

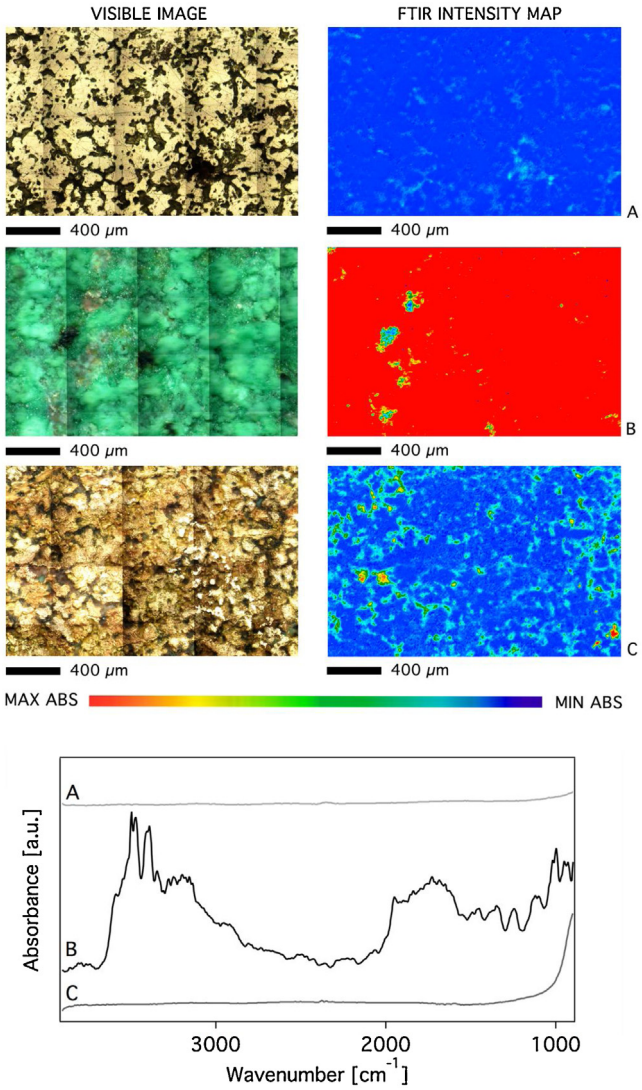

Fig. 7. FTIR 2D Imaging of a bronze mock-up (coin) before artificial aging (A), after artificial aging (B), and after cleaning with an HVPD system loaded with TEPA 3% wt (C). Beside each visible map, the corresponding 2D FTIR map shows the intensity, between 3111 and 3679 cm^{-1}, of the hydroxyl stretching bands of hydrated copper(II) hydroxychlorides (e.g. atacamite/clinoatacamite, common copper corrosion products). All maps have dimensions of 1400 × 2100 μm^2. The bottom panel shows the FTIR Reflectance spectra corresponding to representative pixels (5.5 × 5.5 μm^2) of each 2D Imaging map.

cal look of the masterpiece in times dramatically shorter than the conventional restoration practice (days vs. months).

4. Conclusions

TEPA, a strong Cu(II) chelating agent, was confined in PVA-based HVPDs to allow safe and feasible removal of corrosion products from bronze sculptures. The main effect of uploading the polyamine in the polymer network is to induce the alkaline hydrolysis of acetyl groups in PVA chains, which promotes the association of the chains into more ordered structures. As a result, the viscoelasticity of the HVPDs increases significantly, reducing the time needed for film formation, which fulfills the conservator requirements. The process proceeds up to the formation of a highly elastic gum in one week, while strongly alkaline solutions of hydroxides produced similar effects in much shorter time (e.g. 1 min). The slower process with TEPA was ascribed to the presence of polyamine molecules partially protonated and interacting with acetate ions formed by the alkaline hydrolysis of acetate groups in PVA, which might hinder the association of the PVA chains.

The TEPA-loaded HVPDs have a rheological behavior that allows their homogeneous adhesion on highly textured 3D surfaces hardly accessible by rigid gels. The dispersions were used in applications of 1–2 h, which was enough to remove stubborn degradation patinas that had proved resistant to EDTA. The confinement of the chelating agent inside the PVA matrix allowed the effective and progressive removal of the degradation layers (containing copper(II) hydroxychlorides) from a 16th century Italian bronze masterpiece, bringing back the natural cuprite patina of the historical bronze. 2D FTIR FPA Imaging showed that the removal is homogeneous down to the micron scale, and that no PVA residues are left on the surface. In conclusion, these HVPDs formulations candidate as effective and reliable materials for the cleaning of metal sculptures, overcoming the limitations and risks of traditional dry- and wet-cleaning in the restoration practice. Future perspectives might include the use of these systems to remove thick and disfiguring encrustations from archaeological artworks (potentially including also ceramics and glazed surfaces), preserving the so-called “noble” patina, i.e. the compact passive protective layer formed during the long-term exposure to the environment.

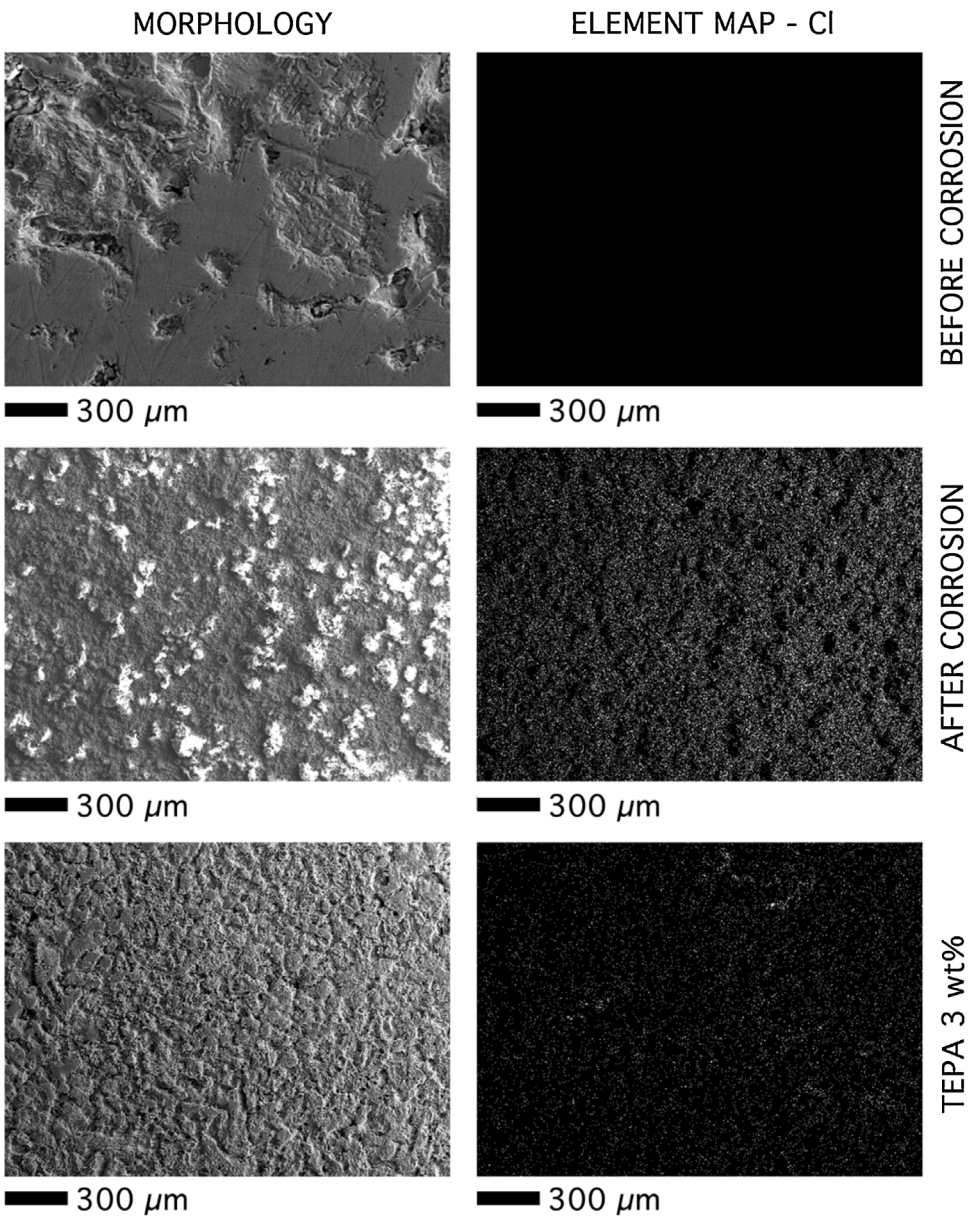

Fig. 8. FEG-SEM images vs. energy dispersive X-ray (EDX) maps of elemental Cl, related with the presence of copper(II) hydroxychlorides (corrosion products). Top row: the surface of a bronze mock-up (coin) before accelerated aging. Center row: the coin surface after aging. Bottom row: the coin surface after removal of corrosion products with an HVPD loaded with TEPA 3% wt.

Fig. 9. (Left Panel) (A) A film of HVPD loaded with TEPA 3% wt lying on a corroded copper surface. The deep blue color is indicative of the TEPA complexing action [36]. (B) Detail showing the feasible peeling of the film off the surface. (Center and Left panels). Benvenuto Cellini, *Perseo libera Andromeda (Perseus frees Andromeda),* 1545-1554, National Museum of Bargello, Florence (IT): detail of the bas-relief surface before and after cleaning with HVPDs loaded with TEPA 3% wt.

Declaration of Competing Interest

The authors declare that they have no known competing financial interests or personal relationships that could have appeared to influence the work reported in this paper.

CRediT authorship contribution statement

Teresa Guaragnone: Investigation, Methodology, Writing - original draft. **Andrea Casini:** Investigation, Methodology, Writing - original draft. **David Chelazzi:** Investigation, Methodology, Writing - original draft. **Rodorico Giorgi:** Conceptualization, Methodology, Investigation, Supervision.

Acknowledgements

The authors acknowledge Ludovica Nicolai ('Restauro e conservazione beni culturali in metallo e leghe' atelier, Florence, Italy) for the cleaning tests on bronze mock-ups and real artifact.Paola D'Agostino and Ilaria Ciseri (Museo del Bargello, Florence, Italy) are also acknowledged for the permission to do tests on the original artifact. Gabriel Maria Ingo (CNR-ISMN, Rome) is gratefully acknowledged for providing the bronze mock-up (coin) and specifications on its composition. Erica Parisi and Raffaello Nardin (CSGI) are acknowledged for the contribution given during some measurements. CSGI and European Union (project NANORESTART, H2020-NMP-21-2014/646063) are acknowledged for financial support.

References

[1] D.A. Scott, Bronze disease: a review of some chemical problems and the role of relative humidity, J. Am. Inst. Conserv. 29 (1990) 193–206, http://dx.doi.org/10.1179/019713690806046064.
[2] G.M. Ingo, C. Riccucci, G. Guida, M. Albini, C. Giuliani, G. Di Carlo, Rebuilding of the burial environment from the chemical biography of archeological copper-based artifacts, ACS Omega 4 (2019) 11103–11111, http://dx.doi.org/10.1021/acsomega.9b00569.
[3] P. Baglioni, D. Chelazzi, R. Giorgi, Nanotechnologies in the Conservation of Cultural Heritage, Springer, Netherlands, 2015, http://dx.doi.org/10.1007/978-94-017-9303-2.
[4] C. Fotakis, D. Anglos, V. Zafiropulos, S. Georgiou, V. Tornari, Lasers in the Preservation of Cultural Heritage: Principles and Applications, Taylor & Francis, 2006, http://dx.doi.org/10.1155/2006/7479.
[5] J.A.L. Domingues, N. Bonelli, R. Giorgi, E. Fratini, F. Gorel, P. Baglioni, Innovative hydrogels based on semi-interpenetrating p(HEMA)/PVP networks for the cleaning of water-sensitive cultural heritage artifacts, Langmuir 29 (2013) 2746–2755, http://dx.doi.org/10.1021/la3048664.
[6] N. Bonelli, D. Chelazzi, M. Baglioni, R. Giorgi, P. Baglioni, Confined aqueous media for the cleaning of cultural heritage: innovative gels and amphiphile-based nanofluids, in: Nanosci. Cult. Herit, Atlantis Press, Paris, 2016, pp. 283–311, http://dx.doi.org/10.2991/978-94-6239-198-7_10.
[7] D. Chelazzi, R. Giorgi, P. Baglioni, Microemulsions, micelles, and functional gels: how colloids and soft matter preserve works of art, Angew. Chem. Int. Ed. 57 (2018) 7296–7303, http://dx.doi.org/10.1002/anie.201710711.
[8] P. Baglioni, E. Carretti, D. Chelazzi, Nanomaterials in art conservation, Nat. Nanotechnol. 10 (2015) 287–290, http://dx.doi.org/10.1038/nnano.2015.38.
[9] P. Baglioni, D. Berti, M. Bonini, E. Carretti, L. Dei, E. Fratini, R. Giorgi, Micelle, microemulsions, and gels for the conservation of cultural heritage, Adv. Colloid Interface Sci. 205 (2014) 361–371, http://dx.doi.org/10.1016/J.CIS.2013.09.008.
[10] R. Mastrangelo, C. Montis, N. Bonelli, P. Tempesti, P. Baglioni, Surface cleaning of artworks: structure and dynamics of nanostructured fluids confined in polymeric hydrogel networks, Phys. Chem. Chem. Phys. 19 (2017) 23762–23772, http://dx.doi.org/10.1039/C7CP02662E.
[11] P. Baglioni, N. Bonelli, D. Chelazzi, A. Chevalier, L. Dei, J. Domingues, E. Fratini, R. Giorgi, M. Martin, Organogel formulations for the cleaning of easel paintings, Appl. Phys. A Mater. Sci. Process. 121 (2015) 857–868, http://dx.doi.org/10.1007/s00339-015-9364-0.
[12] N. Bonelli, G. Poggi, D. Chelazzi, R. Giorgi, P. Baglioni, Poly(vinyl alcohol)/poly(vinyl pyrrolidone) hydrogels for the cleaning of art, J. Colloid Interface Sci. 536 (2019) 339–348, http://dx.doi.org/10.1016/J.JCIS.2018.10.025.
[13] I. Natali, E. Carretti, L. Angelova, P. Baglioni, R.G. Weiss, L. Dei, Structural and mechanical properties of "peelable" organoaqueous dispersions with partially hydrolyzed poly(vinyl acetate)-borate networks: applications to cleaning painted surfaces, Langmuir 27 (2011) 13226–13235, http://dx.doi.org/10.1021/la2015786.
[14] V. Goodship, D. Jacobs, E.O. Ogur, Polyvinyl Alcohol: Materials, Processing and Applications, Smithers Rapra Technology, Shrewsbury, 2005, https://www.worldcat.org/title/polyvinyl-alcohol-materials-processing-and-applications/oclc/765554475. (Accessed 18 September 2019).
[15] C.A. Finch (Ed.), Chemistry and Technology of Water-Soluble Polymers, Springer US, Boston, MA, 1983, http://dx.doi.org/10.1007/978-1-4757-9661-2.
[16] C.M. Hassan, N.A. Peppas, Structure and applications of poly(vinyl alcohol) hydrogels produced by conventional crosslinking or by freezing/thawing methods, in: Biopolym. PVA Hydrogels, Anionic Polym. Nanocomposites, Springer, Berlin Heidelberg, Berlin, Heidelberg, 2000, pp. 37–65, http://dx.doi.org/10.1007/3-540-46414-X_2.
[17] E.I. Parisi, N. Bonelli, R. Giorgi, G.M. Ingo, P. Baglioni, Development of an innovative film-forming cleaning system for the removal of corrosion products from copper alloy artifacts, in: ICOM-CC 18th Triennial Conference Preprints, Copenhagen, 4–8 September, 2017.
[18] H. Burgess, The use of chelating agents in conservation treatments, Pap. Conserv. 15 (1991) 36–44, http://dx.doi.org/10.1080/03094227.1991.9638395.
[19] R.M. Smith, A.E. Martell, Critical Stability Constants: Volume 2: Amines, Springer US, 1975.
[20] N.I. Sax, R.J. Lewis, Hawley's Condensed Chemical Dictionary, Van Nostrand Reinhold, 1987.
[21] M. Abasian, V. Hooshangi, P.N. Moghadam, Synthesis of polyvinyl alcohol hydrogel grafted by modified Fe_3O_4 nanoparticles: characterization and doxorubicin delivery studies, Iran. Polym. J. (English Ed.) 26 (2017) 313–322, http://dx.doi.org/10.1007/s13726-017-0521-5.
[22] N.A. Peppas, E.W. Merrill, Differential scanning calorimetry of crystallized PVA hydrogels, J. Appl. Polym. Sci. 20 (1976) 1457–1465, http://dx.doi.org/10.1002/app.1976.070200604.
[23] M.P. Casaletto, T. De Caro, G.M. Ingo, C. Riccucci, Production of reference "ancient" Cu-based alloys and their accelerated degradation methods, Appl. Phys. A 83 (2006) 617–622, http://dx.doi.org/10.1007/s00339-006-3545-9.
[24] G. Di Carlo, C. Giuliani, C. Riccucci, M. Pascucci, E. Messina, G. Fierro, M. Lavorgna, G.M. Ingo, Artificial patina formation onto copper-based alloys: chloride and sulphate induced corrosion processes, Appl. Surf. Sci. 421 (2017) 120–127, http://dx.doi.org/10.1016/J.APSUSC.2017.01.080.
[25] A. Hebeish, I.I. Abdel-Gawad, I.K. Basily, S. El-Bazza, Degradation of poly(vinyl alcohol) in strongly alkaline solutions of hydrogen peroxide, J. Appl. Polym. Sci. 30 (1985) 2321–2327, http://dx.doi.org/10.1002/app.1985.070300605.
[26] D. Dibbern-Brunelli, T.D.Z. Atvars, I. Joekes, V.C. Barbosa, Mapping phases of poly(vinyl alcohol) and poly(vinyl acetate) blends by FTIR microspectroscopy and optical fluorescence microscopy, J. Appl. Polym. Sci. 69 (1998) 645–655, http://dx.doi.org/10.1002/(SICI)1097-4628(19980725)69:4<645::AID-APP3>3.0.CO;2-J.
[27] W.C. Wilfong, C.S. Srikanth, S.S.C. Chuang, In situ ATR and DRIFTS studies of the nature of adsorbed CO2 on tetraethylenepentamine films, ACS Appl. Mater. Interfaces 6 (2014) 13617–13626, http://dx.doi.org/10.1021/am5031006.
[28] K. Ito, H.J. Bernstein, The vibrational spectra of the formate, acetate, and oxalate ions, Can. J. Chem. 34 (1956) 170–178, http://dx.doi.org/10.1139/v56-021.
[29] E.I. Parisi, N. Bonelli, E. Carretti, R. Giorgi, G.M. Ingo, P. Baglioni, Film forming PVA-based cleaning system for the removal of corrosion products from Cu-based alloys, Pure Appl. Chem. 90 (3) (2017), http://dx.doi.org/10.1515/pac-2017-0204.
[30] S.Z.D. Cheng, Handbook of Thermal Analysis and Calorimetry: Volume 3: Applications to Polymers and Plastics, Elsevier, 2002.
[31] S. Muppalaneni, H. Omidian, Polyvinyl alcohol in medicine and pharmacy: a perspective, J. Develop. Drugs 02 (2013), http://dx.doi.org/10.4172/2329-6631.1000112.
[32] W. Martens, R.L. Frost, P.A. Williams, Raman and infrared spectroscopic study of the basic copper chloride minerals – implications for the study of the copper and brass corrosion and bronze disease, Neues Jahrb. Für Mineral. - Abhandlungen. 178 (2003) 197–215, http://dx.doi.org/10.1127/0077-7757/2003/0178-0197.
[33] G.M. Ingo, G. Guida, E. Angelini, G. Di Carlo, A. Mezzi, G. Padeletti, Ancient mercury-based plating methods: combined use of surface analytical techniques for the study of manufacturing process and degradation phenomena, Acc. Chem. Res. 46 (2013) 2365–2375, http://dx.doi.org/10.1021/ar300232e.
[34] S. Vahur, A. Teearu, P. Peets, L. Joosu, I. Leito, ATR-FT-IR spectral collection of conservation materials in the extended region of 4000-80 cm^{-1}, Anal. Bioanal. Chem. 408 (2016) 3373–3379, http://dx.doi.org/10.1007/s00216-016-9411-5.
[35] G.M. Ingo, S. Balbi, T. de Caro, I. Fragalà, E. Angelini, G. Bultrini, Combined use of SEM-EDS, OM and XRD for the characterization of corrosion products grown on silver roman coins, Appl. Phys. A 83 (2006) 493–497, http://dx.doi.org/10.1007/s00339-006-3533-0.
[36] P. Pulkkinen, J. Shan, K. Leppänen, A. Känsäkoski, A. Laiho, M. Järn, H. Tenhu, Poly(ethylene imine) and Tetraethylenepentamine as protecting agents for metallic copper nanoparticles, ACS Appl. Mater. Interfaces 1 (2009) 519–525, http://dx.doi.org/10.1021/am800177d.